

<Original> **An Improved Proton Recoil Telescope
Detector for Fast Neutron Spectroscopy**

Moon Kyu Chung and Hee Dong Kang
Korea Atomic Energy Research Institute, Seoul, Korea

Tong Soo Park
Kyung pook National University, Daegu, Korea

(Received January 16, 1973)

Abstract

For fast neutron spectroscopy in MeV region, a recoil proton telescope detector was designed and constructed so as to increase in detection efficiency without appreciable deterioration in energy resolution by adopting a special type of recoil proton radiator which is a combination of a ring-shaped vertical radiator and a cone-shaped horizontal radiator at a certain geometry. A neutron stopper was built in the detector system to minimize the background due to direct exposure of the Si(Li) detectors to primary incident neutrons. The detection efficiency and the energy resolution calculated at various neutron energies and geometries are given and these characteristics of the detector system were tested by 14.1 MeV neutrons. As the calculation predicted, the relative detection efficiency in case of the combined radiator system is almost 2.2 times of that for a single, ring-shaped vertical radiator system. The calculated energy resolution is 3.7% FWHM, whereas the measured resolution was 3.9% which means resolution broadening of approximately 30% was resulted by introducing a combined radiator system into the telescope. Increase in background less than 40% was also observed.

요 약

MeV 영역의 速中性子分光을 위해 在來의 radiator system을 改良하여 ring-shaped vertical radiator와 cone-shaped horizontal radiator를 共用한 特殊한 recoil proton radiator assembly를 使用함으로써 energy 分解能의 低下없이 檢出效率를 높 이도록 recoil proton telescope detector를 設計·製作하였다. 이 檢出器에는 入射 中性子束에 對한 Si(Li) 檢出器의 直接露出을 避함으로서 background를 減일수 있 도록 入射中性子遮蔽部도 考案 內藏되어 있다. 이 改良된 recoil proton telescope detector의 檢出效率 및 energy 分解能을 中性子 energy 1~15 MeV에 對하여 radiator system과 Si(Li) 檢出器사이의 距離變化에 따라 理論的인 計算值로 導出· 表示하였으며, 實驗的檢證의 例로서 이 거리를 29cm로 하고 中性子 energy를 14.1 MeV로 하였을 때의 檢出器의 諸特性測定結果를 얻어 分析하였다. 測定結果의 分析 에 依하면 理論에서 推定된것처럼 混合型 radiator system을 使用하였을 때의 檢出 效率는 單一 radiator system을 使用한 在來式 檢出器의 檢出效率의 2.2배의 增加 를 보인데 反하여 energy 分解能의 低下는 不過 30%, background의 增加는 約40%

未滿임을 알수가 있었다. 또한 測定에 依한 14.1 MeV 中性子에 對한 energy 分解能은 3.9% FWHM 이었는데, 이는 理論的인 3.7% FWHM 와 거의 完全한 一致를 보이고 있음도 立證되었다.

1. Introduction

Operational principles of nearly all spectrometers for neutrons with energies from 1 MeV to 20 MeV depend on the observation of one of the followings: neutron time-of-flight, recoil protons due to n-p scattering, or reaction products from $\text{He}^3(n,p)\text{H}^3$ or $\text{Li}^6(n,\alpha)\text{H}^3$.

Photographic emulsions and cloud chambers are thick radiator spectrometers with good resolution and good background discrimination, but these advantages are mullified by the tedious measurements of tracks. He^3 counters have an inherent background from He^3 recoils which is serious for neutron energies above 1 MeV. Time-of-flight spectrometers lose their resolution above a few MeV because extremely short flight time is difficult to measure by existing methods. As is well known, proton recoil telescope detector usually consists of a hydrogenous radiator together with two or more counters which are placed in tandem and operated in coincidence, or perhaps anticoincidence, to detect the proton recoiling with a small solid angle to a collimated neutron flux. The use of coincidence techniques gives good discrimination effect against background. When n-p scattering cross section is known, the neutron detection efficiency can be calculated accurately from the composition of the radiator material and the solid angle sustained by the detector. If the detector is energy sensitive, the neutron spectrum can be fairly easily determined from the recoil spectrum. Thus a proton recoil telescope detector has known efficiency and good background discrimination characteristics.

On the other hand it suffers from very low detection efficiency particularly at low energies.

The early telescope detectors consisted of a thin polyethylene radiator and a series of proportional counters. Soon after, various modifications have been made by using a solid scintillator such as NaI (Tl) or CsI (Tl) scintillation counter operating in coincidence with one or more proportional counters. However these types of recoil proton detectors showed poor resolution or low detection efficiency. Since the beginning of the last decade, the semiconductor counter telescope has been successfully used in numerous studies of nuclear reactions induced by 14 MeV neutrons.¹⁻³⁾ It has been demonstrated in these investigations that the semiconductor counter detector, in addition to good energy resolution and excellent stability, ensures good separation of various particles and fast operation, making experiments with high neutron flux possible. However, it has also shown that this telescope detector has a relatively high background due to the large cross section for neutron induced reactions in silicon such as $\text{Si}^{28}(n,p)$ and $\text{Si}^{28}(n,\alpha)$.

Nowadays, the semiconductor telescope detector seems to be one of the most versatile fast neutron detectors if the background can be eliminated and the improvement in detection efficiency can be made. In our present experiments, efforts were made to avoid these difficulties in the design of a telescope detector by introducing a radiator system composed of a ring-shaped vertical radiator and a cone-shaped horizontal radiator and an $E - \frac{dE}{dX}$ detector system.

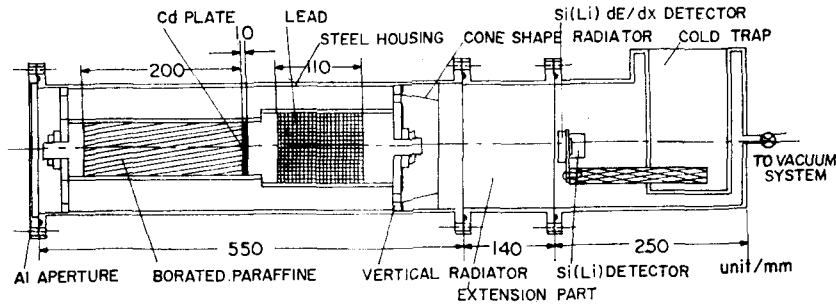


Fig. 1. Schematic drawing of a telescope detector

2. Construction Details of the Telescope Detector

As shown in Fig. 1, the telescope detector consists of essentially five parts: detector shielding, hydrogenous radiator, extension tube, detector holder including a cold finger and $E-\frac{dE}{dX}$ detector. From the geometry of radiators, it is necessary to select incoming fast neutrons within certain small incident angle by placing a collimator on the path of neutrons. Also it is necessary to eliminate the possibility of direct exposure of incoming fast neutrons on to detectors by putting a proper scatterer at the center of neutron beam area. Detector shield has both of these functions. The main constituents of the detector shield are shown in Fig. 1. To stop the neutrons thermalized by the borated paraffine moderator, a thick cadmium plate with 1cm in thickness is put between two steel pipes. The steel pipe filled with lead act as a fast neutron attenuator and a shielding of gamma-rays emitted mainly from preceding steel pipe filled with borated paraffine and a cadmium plate due to neutron capture.

To increase the detection efficiency without appreciable deterioration in energy resolution, particular care was paid for geometry of radiators. Two independent radiators are

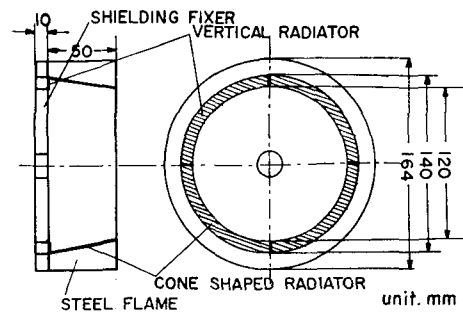


Fig. 2 a. Cross sections of vertical and cone shaped radiator

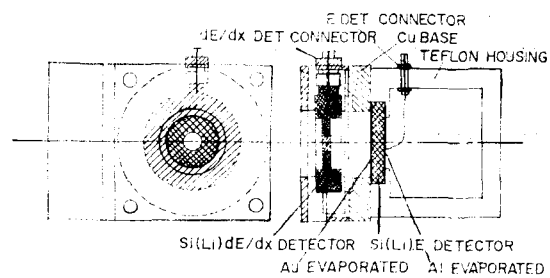


Fig. 2 b. Principle of mounting Si(Li) E- and dE/dx detector

provided: a ring-shaped radiator vertical to the direction of incident neutrons and a cone-shaped radiator of $\sqrt{26}$ cm in length having $\varphi = \tan^{-1} \frac{1}{5}$ respect to direction of incoming neutrons. The vertical radiator with a total area of 40.8cm² is shaped into ring type by fixing it into two concentric steel frames having diameter of 14cm and 12cm respectively. The geometrical arrangement of these two radiators is shown in Fig. 2a. However

this arrangement can be easily modified into a single vertical radiator or a single cone shaped radiator arrangement. These two radiators of different geometries are so arranged that the all neutrons transmitted through the vertical radiator without interaction have opportunities to interact with horizontal cone-shaped radiator to eject protons.

Three extension pipes with different lengths (14, 19 and 29cm) and the same diameter as that of steel housing are provided to vary the distance between the radiator assembly and the detector system to find out the effect of the variation of distance on the resolution and efficiency. By singly replacing the extension pipes, the distance between the radiator assembly and detector system can be varied in steps of 24cm, 29cm and 39cm.

As shown in Fig. 2b, detector assembly consisting of E-and dE/dx detectors are stacked together and mounted on a copper cold finger which is cooled down to liquid nitrogen temperature to suppress the thermal noise. However it should be noted that the experiments reported in this paper were done without dE/dx detector which will be used later for improvement in background discrimination characteristics of the spectrometer.

3. Calculated Detection Efficiency and Resolution

Throughout the calculations, the following semi-empirical formula given by Gammel⁽⁴⁾ was used for the derivation of total scattering cross sections in barns

$$\sigma_T(E) = \frac{3\pi}{1.206E + (-1.8600 + 0.09415E + 0.0001307E^2)^2} + \frac{\pi}{1.206E + (0.4223 + 0.1300E)^2} \quad (1)$$

where the neutron energy E is expressed in MeV at laboratory system. The differential

cross sections in barns in laboratory system is deduced from

$$\sigma(\theta, E) = \frac{\sigma_T(E)\cos\theta}{\pi} \cdot \frac{1 + 2\left(\frac{E}{90}\right)^2 \cos^2 2\theta}{1 + \left(\frac{2}{3}\right)\left(\frac{E}{90}\right)^2} \quad (2)$$

The anisotropy of $n-p$ scattering due to interference between S and D waves was disregarded as its contribution to $\sigma(\theta, E)$ is negligible below 14MeV.

1) Detection Efficiency in Case of a Vertical Radiator

In case of vertical radiator as shown in Fig. 3, the detection efficiency of the telescope detector can be easily calculated in the following way. As seen in the figure, a, b and d denote the diameters of silicon detectors, the distance from a point on the center axis and the distance between the detector and the radiator respectively.

As it is assumed that the collimated parallel neutron beam falls on the radiator

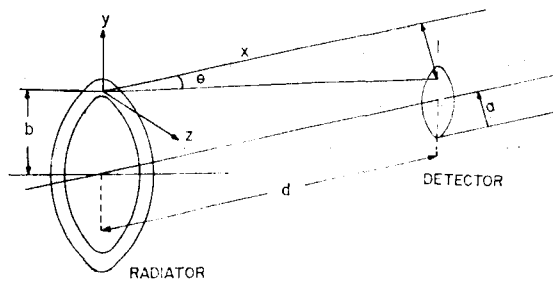


Fig. 3. Basic geometry for the vertical radiator. The symbols are defined in the sections on efficiency and resolution

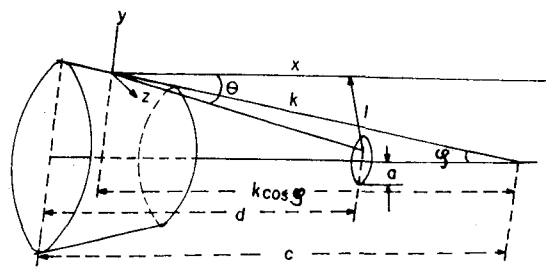


Fig. 4. Basic geometry for the cone-shaped radiator. The symbols are defined in the sections on efficiency and resolution.

vertically, the number of recoil protons with kinetic energy E emitted from an areal element, $ds=2\pi b db$, on the radiator is given

$$\begin{aligned} dn(E) &= N\phi(E) \cdot \sigma(\theta, E) \cdot \Omega ds \\ &= N\phi(E) \cdot \sigma(\theta, E) \Omega \cdot 2\pi b db \end{aligned} \quad (3)$$

where

N : the number of hydrogen atoms per unit area in the radiator

$\phi(E)$: incident neutron flux

Ω : solid angle sustained by the detector to see the point b on the radiator.

As $\sigma(\theta, E)$ and Ω can be expressed in the following forms

$$\sigma(\theta, E) = \frac{\sigma_T(E) \cos\theta}{\pi} = \frac{\sigma_T(E) \cdot d}{\pi(b^2 + d^2)^{\frac{1}{2}}}$$

$$\Omega = \frac{\pi a^2 d}{(b^2 + d^2)^{3/2}} \quad (4)$$

we get

$$dn(E) = \frac{2\pi N\phi(E)\sigma_T(E)a^2 d^2 b db}{(b^2 + d^2)^2} \quad (5)$$

By integrating above equation over the whole area of the radiator, the total number of recoil protons with energy E is expressed as

$$\begin{aligned} n(E) &= 2\pi a^2 d^2 N\phi(E)\sigma_T(E) \int_{b_1}^{b_2} \frac{b}{(b^2 + d^2)^2} db \\ &= \pi a^2 d^2 \cdot \left[\frac{1}{b_1^2 + d^2} - \frac{1}{b_2^2 + d^2} \right] \cdot N\sigma_T(E)\phi(E) \end{aligned} \quad (6)$$

For our telescope, this expression becomes as

$$n(E) = A \cdot N\sigma_T(E)\phi(E) \quad (7)$$

and each numerical values is given as follows:

$a=0.9\text{cm}$, $b_1=6\text{cm}$, $b_2=7\text{cm}$, $d=10\text{cm}$, 24cm , 29cm , 39cm . By putting these values into the equ. (6), following values of A are obtained for different d : $A=0.16325$, 0.04982 , 0.03564 and 0.02058 .

As the mylar film (hydrogen content being $1/24$) of thickness $1.04\text{mg}/\text{cm}^2$ is used as radiators, the number of hydrogen atoms per unit area is 2.15×10^{19} and this value yields following results:

$$n(E) = 3.510 \times 10^{-5} \cdot \sigma_T(E) \cdot \phi \quad \text{when } d=10\text{cm}$$

$$n(E) = 1.071 \times 10^{-6} \cdot \sigma_T(E) \cdot \phi \quad \text{when } d=24\text{cm}$$

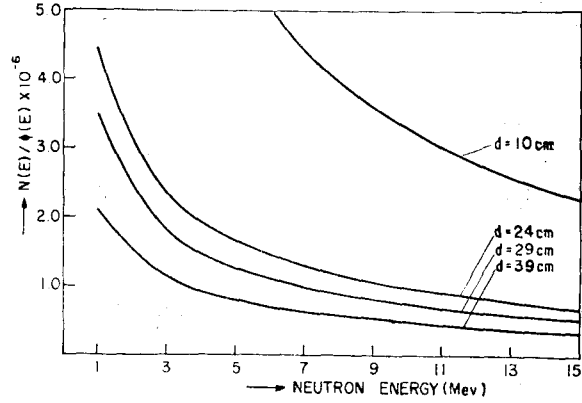


Fig. 5. The efficiency of the telescope detector using the vertical radiator

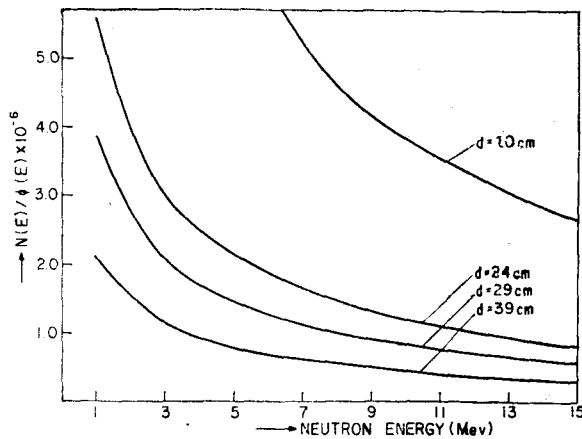


Fig. 6. The efficiency of the telescope detector using the cone-shaped radiator

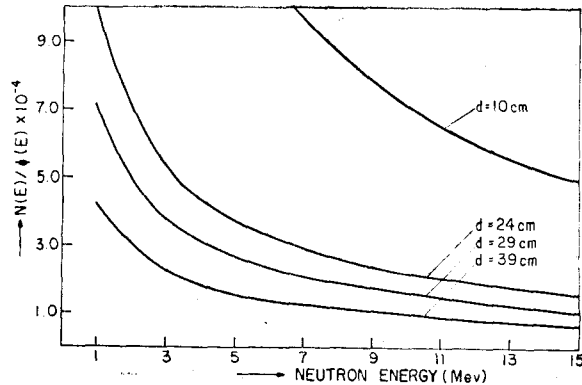


Fig. 7. The efficiency of the telescope detector using the combined radiator

$n(E) = 7.663 \times 10^{-7} \cdot \sigma_T(E) \cdot \phi$ when $d = 29\text{cm}$

$n(E) = 4.425 \times 10^{-7} \cdot \sigma_T(E) \cdot \phi$ when $d = 39\text{cm}$.

The ratio, $n(E)/\phi$, is computed for mylar radiator and shown in Fig. 5.

2) Detection Efficiency in Case of a Cone-shaped Radiator

As seen in Fig. 4, a variable denoted by k was chosen as the distance between a point on cone-shaped radiator and the point where the extrapolated line from the radiator surface crosses the center axis of the detector system. Then the total number of recoil protons from the areal element, $ds = 2\pi k \cdot \sin^2\varphi dk$, of the radiator is given by

$$dn(E) = N\phi(E) \cdot \sigma(\theta, E) \cdot 2\pi k \cdot \sin^2\varphi dk \quad (8)$$

where

$$\sigma(\theta, E) = \frac{\sigma_T(E) \cdot (d - c + k \cdot \cos\varphi)}{\pi \sqrt{k^2 \sin^2\varphi + (d - c + k \cdot \cos\varphi)^2}} \quad (9)$$

$$\Omega = \frac{\pi a^2 (d - c + k \cdot \cos\varphi)}{[k^2 \sin^2\varphi + (d - c + k \cdot \cos\varphi)^2]^{3/2}} \quad (10)$$

From above relations, following formula is obtained for $dn(E)$:

$$dn(E) = 2\pi a^2 N \phi(E) \cdot \sigma_T(E) \sin^2\varphi \frac{(d - c + k \cdot \cos\varphi)^2 k dk}{[k^2 \sin^2\varphi + (d - c + k \cdot \cos\varphi)^2]^2} \quad (11)$$

Therefore the total number of recoil protons is given by

$$n(E) = 2\pi a^2 N \sin^2\varphi \cdot \phi'(E) \cdot \sigma_T(E) \times \int_{k_1}^{k_2} \frac{(d - c + k \cdot \cos\varphi)^2 k dk}{[k^2 \sin^2\varphi + (d - c + k \cdot \cos\varphi)^2]^2}$$

where $k_1 = 30.6\text{cm}$, $k_2 = 35.7\text{cm}$ and $c = 35\text{cm}$ in the present geometry. For each values of d , following results are obtained.

$n(E) = 4.065 \times 10^{-6} \sigma_T(E) \cdot \phi'$ when $d = 10\text{cm}$

$n(E) = 1.300 \times 10^{-6} \sigma_T(E) \cdot \phi'$ when $d = 24\text{cm}$

$n(E) = 9.045 \times 10^{-7} \sigma_T(E) \cdot \phi'$ when $d = 29\text{cm}$

$n(E) = 5.022 \times 10^{-7} \sigma_T(E) \cdot \phi'$ when $d = 39\text{cm}$.

The ratio, $n(E)/\phi'(E)$, is computed for the mylar film of 1.04mg/cm^2 in thickness and the resulted values are shown in Fig. 6.

3) Detection Efficiency in Case of a Combined Radiator

In Case of combined radiator system, the

neutrons which passed through the vertical radiator without interaction have possibilities to react [with the cone-shaped radiator. Therefore the total number of recoil protons for the whole radiator system is simply a sum of contributions from each radiator. That is

$$\begin{aligned} n(E)_c &= n(E)_v + n(E)_{\text{cone}} \\ &= 2\pi a^2 \sigma_T(E) N \left(\phi(E) \int_{b_1}^{b_2} \frac{b}{(b^2 + d^2)^2} db \right. \\ &\quad \left. + \phi'(E) \sin^2\varphi \int_{k_1}^{k_2} \frac{(d - c + k \cdot \cos\varphi)^2 k dk}{[k^2 \sin^2\varphi + (d - c + k \cdot \cos\varphi)^2]^2} \right) \end{aligned} \quad (12)$$

where $\phi'(E)$ denotes the neutron flux after passing through the vertical radiator. In Fig. 7, variation of detection efficiency with energy is shown when $\phi(E) \approx \phi'(E)$ is assumed.

4) Calculated Energy Resolution in Case of a Vertical Radiator

The resolution largely depends on the geometry such as finite size of the radiator, detection area of detector assembly and the distance between them. For very thin mylar radiator, we may assume that there is no attenuation of neutron beam in the radiator as already mentioned before. So there will be rectangular distribution of recoil protons with the maximum energy equal to $E_p = E_n \cos^2\theta$. and the minimum energy given by $E_p = E_n \cos^2\theta - X \left(\frac{dE}{dX} \right)$. The energy loss of recoil

protons in the radiator should effect on the resolution in general. However because of the thin mylar films used as radiators, the high incident neutron energy and relatively small scattering angles, this effect can be neglected. And so, the calculation of the energy resolution for a vertical radiator (also for a cone-shaped radiator in section 3-5), it was not considered. But for the future experiments where the thick radiators may be used, the energy loss correction on resolution was made for a combined radiator system as described

in section 3-7 even if its contribution to resolution broadening was small.

For convenience in mathematical analysis, we used a set of rectangular coordinates with the origin at the scattering point on the radiator as shown in Fig. 3. Since $E_n = E_p \cos^2 \theta$, the locus corresponding to constant θ and constant energy forms a cone about the X-axis. The intercept of this cone with the plane of the detector surface is a circle defined by the equation as

$$y^2 + z^2 = d^2 \tan^2 \theta = l^2 \quad (13)$$

However only a part of this circle actually intercepts with a detector and will give rise to a counted event. In the same coordinate system, the equation of the circle formed by the detector edge is given by

$$(y-b)^2 + z^2 = a^2 \quad (14)$$

From equ. (13) and (14), the intercepts of these two circles can be represented by

$$z = \pm \sqrt{l^2 - \frac{(l^2 - a^2 + b^2)^2}{4b^2}} \quad (15)$$

Therefore the length of the arc on detector face due to superposition of these two circles is given by

$$S = \int_{z_1}^{z_2} \sqrt{1 + \left(\frac{dy}{dz}\right)^2} dz$$

where $z_1 = -z_2 = \sqrt{l^2 - \frac{(l^2 - a^2 + b^2)^2}{4b^2}}$ and

$\left(\frac{dy}{dz}\right)^2 = \frac{z^2}{l^2 - z^2}$. Finally following relation can be obtained

$$S = 2l \sin^{-1} \left(\frac{\sqrt{4b^2 l^2 - (l^2 - a^2 + b^2)^2}}{2bl} \right) \quad (16)$$

However for proper evaluation of S, two additional factors should be considered. The first is the number of scattering events on a circle of radius b and the second is the differential scattering cross section. All points on a ring at constant b will contribute to the same extent. The differential cross section for hydrogen is proportional to $\cos \theta$. So we can take these factors into account by

multiplying S by b and $\cos \theta$. Then we get

$$S' = 2bl \cos \theta \sin^{-1} \left(\frac{\sqrt{4b^2 l^2 - (l^2 - a^2 + b^2)^2}}{2bl} \right) \quad (17)$$

In equ. (17) let choose b and then let l run over all possible values ($b+a \geq l \geq b-a$), obtaining a curve giving S' , versus θ . This process should be continued until all the values of b are covered. By integrating all the individual curves, we finally obtain the resolution function, $f(\theta)_{ver}$. The resolution function, $f(\theta)$, was thus obtained as a function of angle θ but can be easily converted into the function of proton energy E_p by utilizing the relation, $E_p = E_n \cos^2 \theta$ and $f(\theta)$. The mean scattering angles were found to be 33.05° , 15.15° , 12.80° and 9.35° corresponding to $d=10\text{cm}$, 24cm , 29cm and 39cm respectively. The resolution function is shown in Fig. 8 when $d=29\text{cm}$.

5) Calculated Energy Resolution in Case of a Cone-shaped Radiator

By adopting the same coordinate system shown in Fig. 4, following relation can be obtained.

$$y^2 + z^2 = (d-c+k \cos \varphi)^2 \tan^2 \theta = l^2$$

$$(y-k \sin \varphi)^2 + z^2 = a^2$$

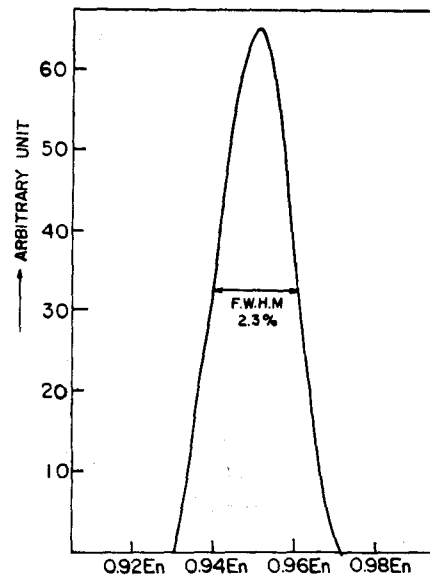


Fig. 8. The geometric resolution function for using the vertical radiator

Therefore intercepts of the two circles are given by

$$z = \pm \sqrt{\frac{l^2 - l^2(a^2 + k^2 \sin^2 \varphi)^2}{4k^2 \sin^2 \varphi}}$$

and the following expressions for S and S' are resulted:

$$S = \int_{z_1}^{z_2} \sqrt{1 + \left(\frac{dy}{dz}\right)^2} dz = \int_{z_1}^{z_2} \sqrt{\frac{l^2}{l^2 - z^2}} dz \quad (18)$$

$$S' = 2kl \sin \varphi \cdot \cos \theta \sin^{-1} \times \sin^{-1} \left(\frac{\sqrt{4k^2 l^2 \sin^2 \varphi - (l^2 - a^2 + k^2 \sin^2 \varphi)^2}}{2kl \sin \varphi} \right) \quad (19)$$

From equ. (19), mean scattering angles of 16.63°, 14.35° and 10.23° were resulted and the resolutions(FWHM) of 3.35%, 2.90% and 1.5% were obtained when $d=24\text{cm}$, 29cm and 39cm respectively. The resolution function, $f(\theta)_{\text{cone}}$, is deduced as shown in Fig. 9 when $d=29\text{cm}$.

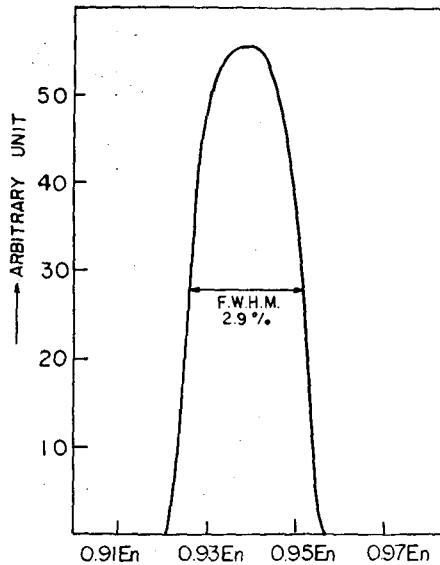


Fig. 9. The geometric resolution function for using the cone-shaped radiator

6) Calculated Energy Resolution in Case of a Combined Radiator

The resolution function, $f(\theta)_{\text{com}}$, in case of combined radiator can be obtained simply by utilizing the following relation of error propagation:

$$f(\theta)_{\text{com}}^2 = f(\theta)_{\text{ver}}^2 + f(\theta)_{\text{cone}}^2 \quad (20)$$

The resolution function curve was computed

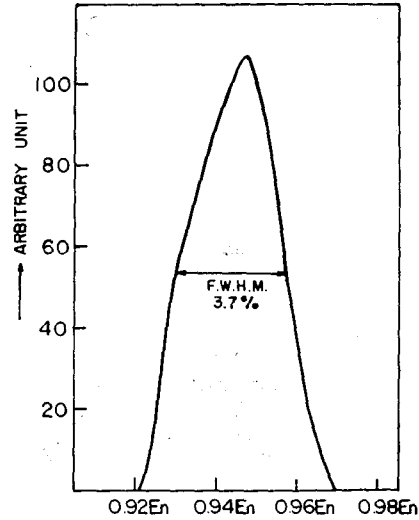


Fig. 10. The geometric resolution function for using the combined radiator

when $d=29\text{cm}$ and is shown in Fig. 10. And mean scattering angles of 15.89°, 13.60° and 9.79° and FWHM of 4.50%, 3.76% and 1.92% were obtained when $d=24\text{cm}$, 29cm and 39cm respectively.

7) Energy Loss Correction

As stated in section 3-4, the resolution mainly depends on the geometries. However recoil protons emitted by neutron collisions in the radiator have to lose a part of their kinetic energies due to the interaction with radiator materials until they come out from it. The maximum energy loss at geometrically

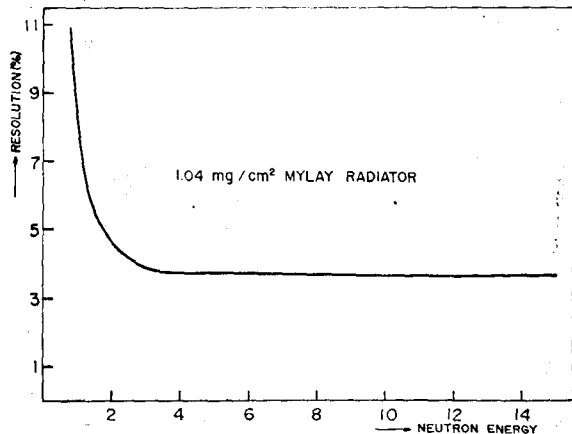


Fig. 11. The overall resolution of the combined radiator telescope detector as a function of E_n

acceptable scattering angles varies with radiator thickness. If the radiator thickness is fixed, the outgoing protons from radiator should have energy distribution which begins with the maximum energy loss and terminates with zero energy loss. For correct evaluation of the energy loss effect on the resolution broadening, energy loss corresponding to every possible length of passage of proton emitted in the radiator at various scattering angles should be taken into account. However as this is very troublesome, we used mean energy loss, $\bar{X}\left(\frac{dE}{dX}\right)$ which is related to E_p and mean scattering angle $\bar{\theta}$ through following equation:

$$E_p = E_n \cos^2 \bar{\theta} - \bar{X} \left(\frac{dE}{dX} \right) \quad (21)$$

where \bar{X} is the mean distance of proton travelled through radiator.

For instance, when $d=29\text{cm}$ in case of combined radiator, $\theta=13.6^\circ$ is resulted. In Fig. 11, the overall resolution function curve corrected for energy loss effect is shown.

4. Experiments

By utilizing $T(D, n) \text{He}^4$ reaction, 14 MeV monoenergetic fast neutrons are generated at the total yield of 10^{10} per second in 4π geometry. As the telescope detector was

placed, to see the target at the angle of 80° respect to the direction of accelerated deuteron beam path, expected kinetic energy of neutrons was 14.1 MeV. The chain of all counting electronics except those for plastic scintillator monitor detector is shown in Fig. 12. This chain of electronics modules is actually constructed for a telescope detector system in which coincidence-sum technique will be applied for the pulses resulted from a dE/dX and E - silicon detector system which will be completed soon at our laboratory enables us to get only a sum peak corresponding to totally absorbed recoil proton energy and discriminate the almost all the background⁵⁻⁷). However at the present experiments, a thin windowed Si(Li) detector with 2.5mm depletion depth fabricated at our laboratory and only a part of this electronics chain was utilized. The resulted pulses from the E -detector are amplified and shaped then directly fed to a 800 channel pulse height analyzer.

As the consumption of accelerator target is very rapid and this brings significant change of neutron flux during the experiments, a plastic scintillation counter was used as a monitor counter with which normalization of spectra to the same number of primary

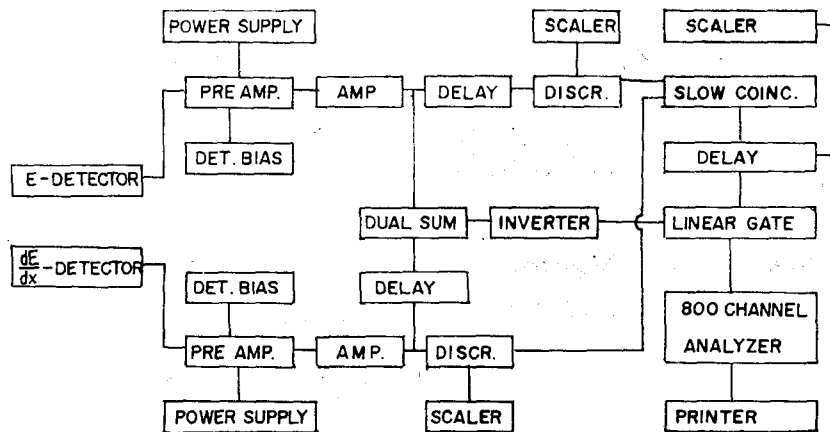


Fig. 12. Block diagram of the electronics system

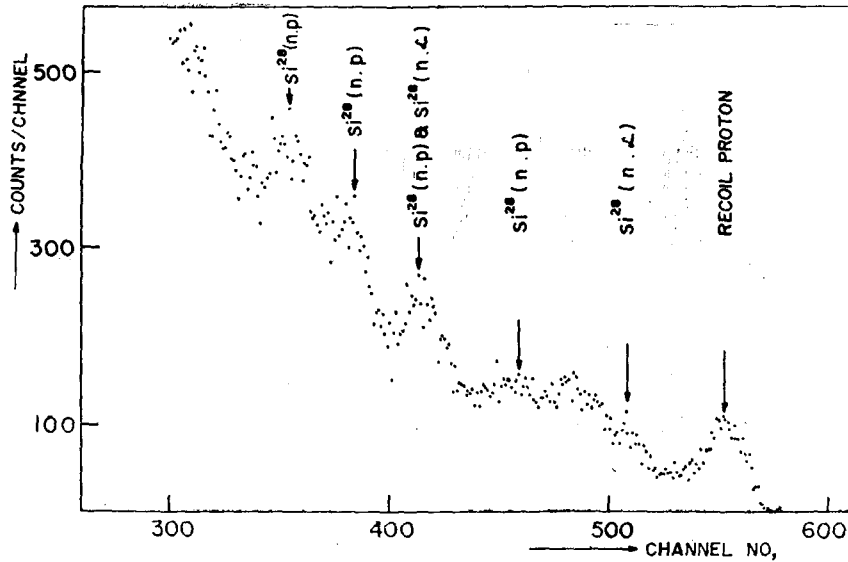


Fig. 13. Proton recoil spectrum using the vertical radiator

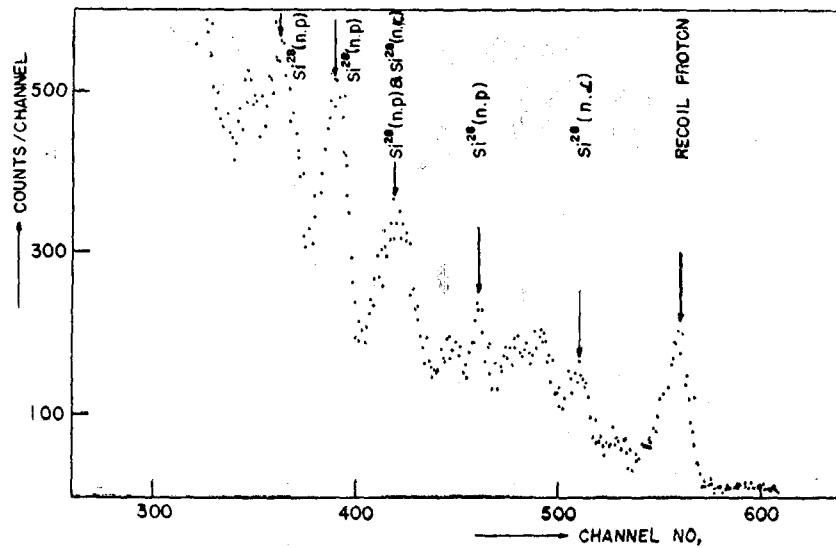


Fig. 14. Proton recoil spectrum using the combined radiator

incident neutrons can be easily made.

To find out experimentally an improvement in detection efficiency and a possible change in energy resolution when a combined radiator is used instead of a single vertical radiator, two spectra of recoil protons were taken and compared under exactly same experimental conditions. These spectra are shown in Fig. 13 and 14.

5. Results and Discussion

By comparing the two spectra shown in

Fig. 13 and 14, it is evident that the increase in detection efficiency of the telescope system employing a combined radiator is almost as much as ≈ 2.2 times of the system where only a single vertical radiator was used. According to the theoretical prediction on the detection efficiencies of both radiator system at $d=29$ cm, the expected increase in detection efficiency should be about 2.16 times because the ratio of number of events detected in both radiator systems is $(7.8174\phi + 9.045\phi') / (7.8174\phi)$ as discussed in sections 3-1~3-3.

There is an excellent agreement between the experimental and theoretical value of ratio of increase in detection efficiency.

The calculated energy resolution is 3.7 % FWHM, whereas the measured resolution was 3.9% which means resolution broadening of approximately 30% was resulted by introducing a combined radiator system into the telescope.

Increase in background less than 40% was also observed. The background seems to be resulted from mainly direct interaction of scattered fast neutron with silicon detector and is distributed in the lower energy region than the recoil proton peak position. However, by setting a discriminator level at a proper position, only the counts under the totally absorbed proton peak can be registered without appreciable loss of counting.

The peak to background ratio is not high enough at present experiments but can be easily improved by using the radiator materials such as polyethylene which has much more

hydrogen atoms per unit volume than mylar and by the proper choice of vertical radiator thickness because a mylar film used for present experiments was found too thin to emit enough protons within the allowed energy loss criteria.

References

- 1) B. Lalovic and V. Ajdacic: Proc. Nucl. Electronics Symp., Paris (1963)
- 2) Kulisic, Cindro, Strohal and Lalovic: Nuclear Physics, 73 (1965)
- 3) V. Ajdacic, M. Cerineo, B. Lalovic, G. Paic, I. Slaus and P. Tomas: Phys. Rev. Letters. 14, 442 (1965)
- 4) Quoted from: S. J. Bame, E. Haddad, J. E. Perry and R. K. Smith: Rev. Sci. Instr., 28, 997 (1957)
- 5) A. C. Melissinos: Experiments in Modern Physics, Academic Press, New York (1966)
- 6) J. B. Marion and J. L. Fowler: Fast neutron Physics, Interscience Publication, Inc., New York (1960)
- 7) G. Alberti, L. Isabella and A. Zambra: Nucl. Instr. and Meth., 95, 413. (1971)